Unipolar resistive switching of Au^+-implanted ZrO_2 films*

Liu Qi(刘琦)[1,2], Long Shibing(龙世兵)[1], Guan Weihua(管伟华)[1], Zhang Sen(张森)[1], Liu Ming(刘明)[1,†], and Chen Junning(陈军宁)[2,†]

(1 Laboratory of Nano-Fabrication and Novel Devices Integrated Technology, Institute of Microelectronics, Chinese Academy of Sciences, Beijing 100029, China)

(2 College of Electronics and Technology, Anhui University, Hefei 230039, China)

Abstract: The resistive switching characteristics of Au^+-implanted ZrO_2 films are investigated. The Au/Cr/Au^+-implanted-ZrO_2/n^+-Si sandwiched structure exhibits reproducible unipolar resistive switching behavior. After 200 write-read-erase-read cycles, the resistance ratio between the high and low resistance states is more than 180 at a readout bias of 0.7 V. Additionally, the Au/Cr/Au^+-implanted-ZrO_2/n^+-Si structure shows good retention characteristics and nearly 100% device yield. The unipolar resistive switching behavior is due to changes in the film conductivity related to the formation and rupture of conducting filamentary paths, which consist of implanted Au ions.

Key words: RRAM; resistive switching; ion implantation; ZrO_2
DOI: 10.1088/1674-4926/30/4/042001 **EEACC:** 2550

1. Introduction

Recently, various new memory devices such as polymer random access memory[1], magnetic random access memory (MRAM)[2], nanocrystal floating gate memory[3], and resistive random access memory (RRAM)[4–15] have been proposed for future nonvolatile memory applications. Among these candidates, RRAM has attracted extensive attention because of its superior characteristics, including high-density integration, low power consumption, fast write/erase operation and long retention time[4]. Reproducible resistive switching was observed in various kinds of materials such as ferromagnetic materials[5], organic materials[6], doped perovskites[7] and binary transition metal oxides[4,8–15]. Among these materials, binary transition metal oxides have the advantage of a simple structure, an easy fabrication process and compatibility with complementary metal-oxide semiconductor (CMOS) technology[4]. Up to now, various models for explaining the switching mechanism in binary transition metal oxides have been proposed. These include formation and rupture of metallic filaments[7–12], Schottky barriers with interface states[13], and trap charging and discharging[15]. However, the exact switching mechanism has not yet been clearly understood. In our previous work, we demonstrate that intentionally introduced external traps in ZrO_2 films can significantly improve the performance, including the device yield[15] and the resistance ratio (high resistive state or low resistive state)[16]. These performance improvements were shown to be due to a more uniform and homogeneous trap concentration.

Ion implantation is a feasible way for introducing impurities and controlling their uniformity. In this letter, we fabricate an Au/Cr/Au^+-implanted-ZrO_2/n^+-Si sandwiched structure by ion implantation. Reproducible unipolar resistive switching is observed and the underlying mechanism of this switching behavior is studied.

2. Experimental setup

The resistive switching memory devices were fabricated on an n^+ silicon wafer (3.5×10^{-3} Ω·cm) after chemical cleaning. The device fabrication steps are as follows: First, a 70 nm ZrO_2 film was deposited by electron beam evaporation at a base pressure of 2.6×10^{-6} Torr and a deposition rate of 1 Å/s. After deposition, the film was subjected to rapid thermal annealing treatment at 800 °C for 120 s in a N_2 gas stream (2.5 L/min). Second, Au^+ was implanted into the ZrO_2 film at a dose of 1×10^{11} cm^{-2} using an energy of 50 keV and follow by annealing at 400 °C for 5 s in N_2 to activate the Au ions. Finally, the top electrodes of 10 nm thick Cr and 50 nm thick Au were evaporated. All the top electrodes were defined as squares (area ranging from100×100 μm^2 to 1000×1000 μm^2) after the lift-off process. To investigate the role of Au^+ in the resistive switching phenomenon, control samples without Au^+implantation (un-implanted samples) were simultaneously fabricated. All current–voltage (I–V) characteristics of the fabricated devices were measured under ambient condition using a Keithley 4200 semiconductor characterization system. During electrical measurements, DC voltages were applied between the top electrode (Cr/Au) of the device and the grounded bottom electrode (n^+-Si).

3. Results and discussion

Figures 1(a) and 1(b) show the typical I–V characteristics of the Au/Cr/Au^+-implanted-ZrO_2/n^+-Si (namely the Au^+-implanted samples) sandwiched structure in semi-logarithmic

* Project supported by the State Key Development Program for Basic Research of China (No. 2006CB30276) and the National Natural Science Foundation of China (Nos. 90607022, 90401002, 60506005).

† Corresponding author. Email: liuming@ime.ac.cn, jnchen@ahu.edu.cn

Received 5 September 2008, revised manuscript received 13 December 2008

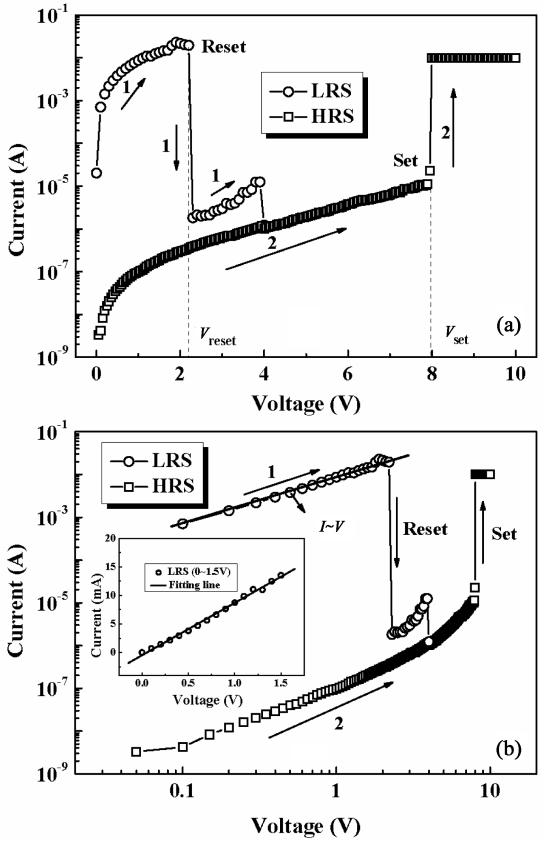

Fig. 1. Typical *I*–*V* characteristics of the Au^+-implanted samples in (a) semi-logarithmic scale and (b) logarithmic scale. Arrows indicate the sweeping directions. The inset shows the *I*–*V* curve at low voltage in the LRS branch. All curves were measured using 800×800 μm^2 cells.

scale and logarithmic scale, respectively. Unlike most of the undoped transition-metal-oxides-based devices[8−12], the Au^+-implanted samples do not need electroforming to develop resistance switching. The initial resistance of Au^+-implanted samples is approximately 10^4 Ω at 0.7 V read voltage and the device is in the on-state. When a positive sweeping voltage (0–4 V) is applied to the top electrode, a sudden drop in current appeared at a voltage that we will call reset voltage, V_{reset}, and the device switches from the low resistance state (LRS) to the high resistance state (HRS), as shown in Fig. 2(a). This sudden current drop defined the "reset" process. Then, by further increasing the applied positive voltage (0–10 V) with a current compliance of 10 mA, an abrupt increase of current appeared at the set voltage, V_{set}, and the device switches from the HRS to the LRS. This current increase defines the "set" process. The reversible resistive switching cycle can be traced hundreds of times. Using a readout voltage of 0.7 V, the typical resistances of the LRS and the HRS of Au^+-implanted samples are $\sim 10^3$ and $\sim 10^7$ Ω, respectively. The resistance ratio (R_{off}/R_{on}) of Au^+-implanted samples can be larger than four orders of magnitude under a 0.7 V readout bias. Almost every device under test shows the same reproducible switching behavior, and the device yield is nearly 100%. In contrast, the initial resistance of the unimplanted sample is $\sim 10^9$ Ω under a

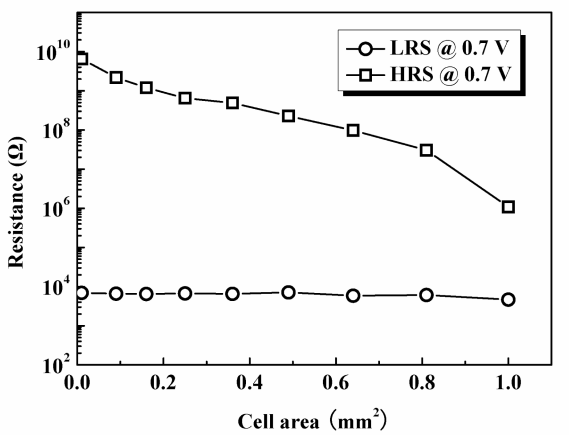

Fig. 2. Resistance of Au^+-implanted samples as a function of cell area (100×100 μm^2–1000×1000 μm^2) for both LRS and HRS. The resistance was recorded at 0.7 V readout voltages.

0.7 V read voltage. During the test of unimplanted cells, about half of the cells show an unstable and noisy switching behavior, and the other half show bipolar switching phenomenon as reported in our previous work[16]. The different resistive switching characteristics of the implanted and unimplanted samples imply that the implanted Au ions in the ZrO_2 films effectively reduce the device-to-device performance spread, and thus increase the device yield because of the more uniform and homogeneous trap concentrations.

According to the experimental results, there are two reasons that the resistive switching phenomenon of the Au^+-implanted samples can be attributed to the filament conductive mechanism. On the one hand, the Au^+-implanted samples show Ohmic behavior in the low voltage (0–1.5 V) LRS branch, which can be seen from the inset of Fig. 1(b). One models that could explain the Ohmic behavior is the formation of conducting filaments throughout the insulating film[11]. On the other hand, the LRS resistivity of the Au^+-implanted samples is independent of cell area, as shown in Fig. 2; an observation that was also made by another group working with Cu:MoO_x[10]. The resistance of LRS is insensitive to the cell sizes, indicating that most current flows through a few localized conducting filamentary paths in the insulator. As seen in Fig. 2, the HRS resistivity is reduced when the cell area is increased, indicating that the Au^+-implanted samples have a sufficient sensing margin when the device is scaled down.

The fact that the Au^+-implanted samples initially are in the low resistance state while the un-implanted samples are initially in the high resistance state, suggests that preformed filamentary conductive paths existed in the Au^+-implanted film. Hence, we believe that the intentionally introduced Au impurities play an important role in forming conducting filamentary paths. When a positive voltage is applied to the top electrode, the current is mainly conducted by these conducting filamentary paths. The generated heat in the conducting filamentary paths and the resulting localized temperature increase eventually results in a rupture of the filaments. In this case, the current drops and the device switches from the LRS to the HRS. According to Ref. [17], implanted metal or

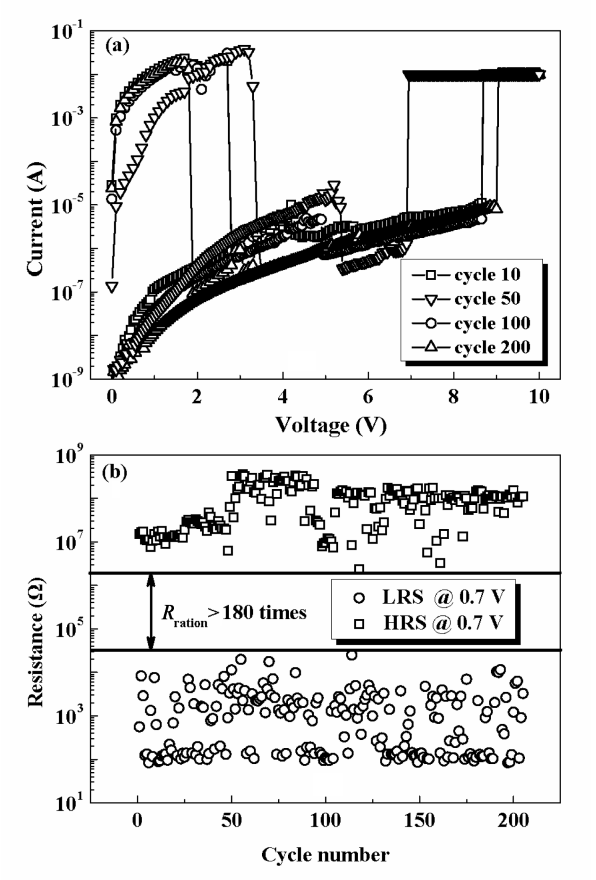

Fig. 3. (a) Continuous *I–V* curve for 10, 50, 100, and 200 cycles; (b) Resistance of the Au^+-implanted samples in the LRS and HRS after 200 cycles. All data measured on $800 \times 800\ \mu m^2$ cells.

oxygen ions in transition metal oxides preferentially precipitate at extended defects such as grain boundaries and dislocations. Likewise, in our samples Au ions can move and rearrange around the ZrO_2 grain boundaries under the high electric field to form local conducting paths. These local conducting paths form when the voltage is increased to V_{set}, which is similar to the mechanism proposed by Choi *et al*. to explain the forming of conducting filaments for TiO_2[9]. In this case, the current steeply increases and the device switches from HRS to LRS.

For further analysis, the stability and retention characteristics of the Au^+-implanted samples were measured to elucidate the potential for their application in nonvolatile memory devices. Figure 3(a) shows the continuous *I–V* curves for 10, 50, 100, and 200 cycles. As can be seen in Fig. 3(a), the shapes of the *I–V* curves remain almost unchanged after 200 cycles. Figure 3(b) shows the resistance of Au^+-implanted samples in the HRS and LRS versus the number of switching cycles at 0.7 V reading voltage. As shown, the ratio of the resistances between the different states is greater than 180 after 200 switching cycles, indicating the excellent device stability.

Figure 4 shows the variation of the resistance in the HRS and LRS with time. For this test, we first obtained on and off states by applying DC voltage switching (0–4 V) and (0–10 V), respectively. Then the resistance of the LRS or HRS was recorded at a constant readout voltage (+ 0.7 V) every 60 s.

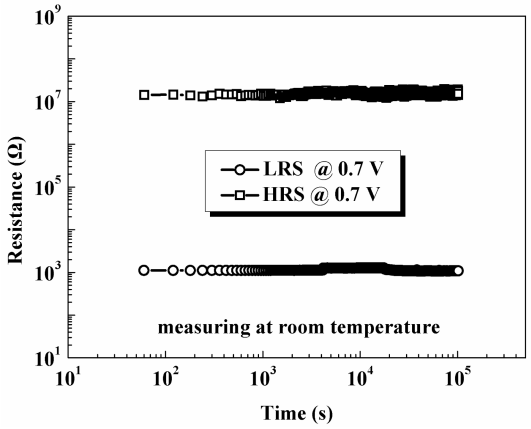

Fig. 4. Resistance of Au^+-implanted sample in the LRS and HRS at constant 0.7 V readout voltage measured for 10^5 s. All data measured on a $800 \times 800\ \mu m^2$ cell.

As can be seen in Fig. 4, no significant changes in the resistances of the LRS and HRS can be observed at room temperature for 10^5 s. This result indicates that the device has stable retention characteristics as needed for their application in nonvolatile memory devices.

4. Conclusion

In conclusion, the Au/Cr/Au^+-implanted-ZrO_2/n^+-Si structure was fabricated and investigated to evaluate its potential for nonvolatile memory applications. It was found that the Au^+-implanted samples exhibited more stable, reproducible resistive switching behavior and a higher device yield than the unimplanted samples. Additionally, the Au^+-implanted samples show good stability and stable retention characteristics over time. This suggests that Au^+-implanted-ZrO_2 films are highly promising with regard to a potential application in future nonvolatile resistive switching memory devices. The resistive switching behavior of Au^+-implanted samples is believed to be due to the formation and rupture of filamentary conductive paths formed by the implanted Au ions.

References

[1] Ma L, Pyo S, Ouyang J, et al. Nonvolatile electrical bistability of organic/metal-cluster/organic system. Appl Phys Lett, 2003, 82(9): 1419

[2] Worledge D C, Abraham D W. Conducting atomic-force-microscope electrical characterization of submicron magnetic tunnel junctions. Appl Phys Lett, 2003, 82(25): 4522

[3] Hanafi H I, Tiwari S, Khan I. Fast and long retention-time nanocrystal memory. IEEE Trans Electron Devices, 1996, 43(9): 1553

[4] Baek I G, Lee M S, Seo S, et al. Highly scalable Non-volatile resistive memory using simple binary oxide driven by asymmetric unipolar voltage pulses. IEDM Tech Dig, 2004: 587

[5] Liu S Q, Wu N J, Ignatiev A. Electric-pulse-induced reversible resistance change effect in magnetoresistive films. Appl Phys Lett, 2000, 76(19): 2749

[6] Ma L, Pyo S, Ouyang J, et al. Nonvolatile electrical bistability of organic/metal-nanocluster/organic system. Appl Phys Lett, 2003, 82(9): 1419

[7] Lin C C, Tu B C, Lin C C, et al. Resistive switching mechanisms of V-doped $SrZrO_3$ memory films. IEEE Electron Device Lett, 2006, 27(9): 725

[8] Seo S, Lee M J, Seo D H, et al. Reproducible resistance switching in polycrystalline NiO films. Appl Phys Lett, 2004, 85(23): 5655

[9] Choi B J, Jeong D S, Kim S K, et al. Resistive switching mechanism of TiO_2 thin films grown by atomic-layer deposition. J Appl Phys, 2005, 98(3): 033715

[10] Lee D, Seong D J, Choi H J, et al. Excellent uniformity and reproducible resistance switching characteristics of doped binary metal oxides for non-volatile resistance memory applications. IEDM Tech Dig, 2006: 346733

[11] Dearnaley G, Stoneham A M, Morgan D V. Electrical phenomena in amorphous oxide films. Rep Prog Phys, 1970, 33: 1129

[12] Wu X, Zhou P, Li J, et al. Reproducible unipolar resistance switching in stoichiometric ZrO_2 films. Appl Phys Lett, 2007, 90(18): 183507

[13] Lee D, Choi H, Sim H, et al. Resistance switching of the non-stoichiometric zirconium oxide for nonvolatile memory applications. IEEE Electron Device Lett, 2005, 26(9): 719

[14] Lin C Y, Wu C Y, Wu C Y, et al. Effect of top electrode material on resistive switching properties of ZrO_2 film memory devices. IEEE Electron Device Lett, 1999, 28(5): 366

[15] Guan W, Long S, Jia R, et al. Nonvolatile resistive switching memory utilizing gold nanocrystals embedded in zirconium oxide. Appl Phys Lett, 2007, 91(6): 062111

[16] Liu Q, Guan W, Long S, et al. Resistive switching memory effect of ZrO_2 films with Zr^+ implanted. Appl Phys Lett, 2008, 92(1): 012117

[17] Szot K, Speier W, Carius R, et al. Localized metallic conductivity and self-healing during thermal reduction of $SrTiO_3$. Phys Rev Lett, 2002, 88(7): 075508